Undergraduate Research Thesis

# Thin-film Hybrid Perovskite Solar Cell: Observations, Comparisons and Mechanisms on the Effects of Gamma-Ray Irradiation

Zeyuan Xu

Department of Electrical and Computer Engineering

The Ohio State University

Advisor: Lei Cao

Department of Mechanical and Aerospace Engineering

Co-advisor: Paul Berger

Department of Electrical and Computer Engineering

# Contents

# Abstract

Perovskite solar cells (PSC) represents a new promising solar technology with great prospects. Much of research has been done to study and enhance the photovoltaic performance and so far, a power conversion efficiency (PCE) exceeding 22.1% has been reached. However, the stability of perovskites remains a major concern for commercialization. In this work, we report a comprehensive study of PSCs under continuous gamma-ray radiation with irradiation time up to 1,535 h and total dose of 2.3 Mrad.

We performed thermal admittance spectroscopy (TAS) on the irradiated devices and found that gamma-ray radiation hardly induces trap states by introduction of crystal point defects. We compared the radiation stability of both p-i-n and n-i-p type of PSC devices and found that p-i-n PSC devices are highly robust to gamma-ray irradiation while the n-i-p PSC devices reduced their PCE by more than 35%. The in-situ measurements indicate that perovskite has features of self-healing to recover from the early degradation caused by gamma-ray irradiation. The post-irradiation evaluation reveals that the perovskite device with p-i-n structure could retain the PCE at 94.6% after correction of the Indium Tin Oxide (ITO) transmittance loss. These observations demonstrate that PSCs show impressive radiation stability against high-energy gamma-ray irradiation and can maintain electrical properties and physical structures in the long term. Th is study is the first to conduct systematical investigation of the effects of gamma-ray irradiation on the perovskite devices, which indicates their potential for future outer space applications.

# Introduction

Perovskite is a typical oxide mineral with the structure resembling calcium titanium oxide (CaTiO3). In the past few decades, several studies were performed on the perovskite solar cell (PSC), given its intrinsic advantages of strong solar absorption, low material cost and simple fabrication process [1], which makes it a suitable substitute for the traditional silicon solar cells. Within a short period of research, PSC quickly achieved an impressive increase in power conversion efficiency (PCE), from 3.8% [2] in 2009 to 22.1% [3] in 2017. However, the stability and lifetime of PSC devices remain questionable and hinder its real-world application. The perovskite layer was found susceptible and degraded at different levels when exposed to oxygen, humidity, heat, and illumination [4]. Hence, many efforts are made in optimizing the PSC fabrication process to enhance the stability. A recent report [5] showed that a PSC based on $SnO_2$ with modified device architecture can maintain over 94% of its peak performance after 1000 h exposure to ambient air environment.

The performance of PSC devices is evaluated based on four important parameters, the maximum power output, short-circuit current ($I_{SC}$), open-circuit voltage ($V_{OC}$), and fill factor (FF). They are obtained from their I-V characteristics. Maximum power output is the maximum power ($P_m$) generated by PSC at a particular point in the I-V curve, with the current and voltage marked as $I_m$ and $V_m$. Given the light power incident ($P_{in}$) on the PSC, the PCE [5] can be calculated by:

$$\eta = \frac{P_m}{P_{in}} = \frac{I_m V_m}{P_{in}} = \frac{I_{SC} V_{OC} FF}{P_{in}} \quad (1)$$

, where FF can be calculated by:

$$FF = \frac{P_m}{P_T} = \frac{P_m}{I_{SC} V_{OC}} = \frac{I_m V_m}{I_{SC} V_{OC}} \quad (2)$$

, where $P_T$ is the theoretical maximum power, which is the product of $I_{SC}$ and $V_{OC}$.

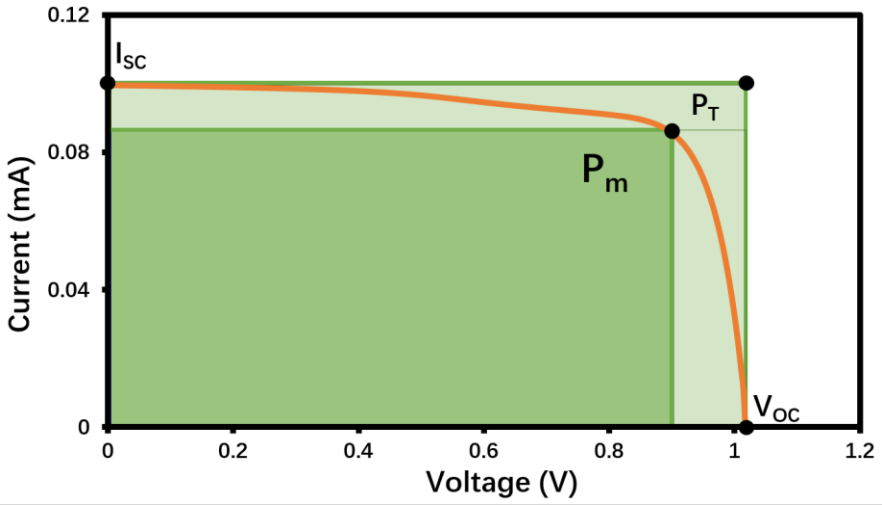


*Figure 1: Typical current-voltage characteristics for a light current of a PSC. Important parameters are included: $I_{SC}$, $V_{OC}$, $P_T$, and $P_m$.*

Fill factor plays a crucial role in identifying the quality of a PSC. As shown in Figure 1, it compares the maximum output power to the theoretical maximum power ($P_T$), which characterizes how "square" the I-V curve of the solar cell is. Such squareness represents the ability of a solar cell to convert the photogenerated carriers into electricity. A perfect square I-V curve will give a 100% FF, meaning that the current generated stayed constant at the maximum value as the applied voltage varies from $V_{OC}$ to zero. However, a perfect 100% FF is impossible to reach. [6] For a normal organic solar cell, the FF ranges from 50% to 70%, depending on [7] the active area of the device, [8] interface between buffer layer active layer etc.

Several studies were performed to reveal the effects of proton, electron and x-ray irradiation on perovskite [9 - 11]. [10] Miyazawa et. al. irradiated 1-MeV electrons on perovskite solar cells and found that the device retained 93% of its peak performance even after irradiation with a fluence of $1 \times 10^{16}$ $cm^{-2}$. Experiments conducted by Lang et. al. [9] indicated a decrease in short-

circuit current ($J_{SC}$) of only 20% in perovskite solar cells exposed to a proton fluence of $1 \times 10^{13}$ $cm^{-2}$. The perovskite also self-healed with recovery on fill factor and open-circuit voltage ($V_{OC}$) after proton irradiation. [11] The effects of soft x-ray exposure on perovskites were investigated by Motoki et. al. who reported that soft x-ray irradiation resulted in evaporation of perovskite surface with residual elements in the form of crystalline $PbI_2$. However, to the best of authors' knowledge, no comprehensive study was performed to test the response of perovskite to gamma-ray radiation. [12] On one hand, large amounts of gamma rays produced when the galactic cosmic rays, mainly comprising protons and alpha particles, undergo nuclear interactions with the constituent nuclei of the spacecraft, poses a challenge to the perovskite materials for their long-term application in space solar cells. On the other hand, [13] organic-inorganic halide perovskites revealed great prospects in radiation detection due to their advantages of large mobility-lifetime product and simple crystal growth while such application strictly forbids performance degradation caused by different levels of radiation. Therefore, it is valuable to examine the stability of perovskite devices in the presence of high-dose gamma-ray radiation.

In this paper, we conducted a comprehensive study of the solar cells based on organohalide lead perovskite. First, multiple p-i-n and n-i-p PSC devices were tested under gamma rays for comparison. Then, a typical p-i-n PSC device was exposed to continuous light and radiation for 1,535 h with a total radiation dose of 2.3 Mrad. The studies performed comprise pre-irradiation characterizations, in-situ radiation measurements, and post-irradiation analysis. The experimental results demonstrated the radiation stability of our PSC devices under gamma-ray irradiation. The mechanisms behind the changes in the electrical characteristics and physical structure of our perovskite solar cells caused by gamma-ray irradiation are explained.

# Experiment

## Device Fabrication

Patterned ITO substrates were cleaned by ultrasonication with soap, acetone and isopropanol. The hole transport layer poly (bis(4-phenyl) (2,4,6-trimethylphenyl)amine) (PTAA) with a concentration of 2 $mg \cdot ml^{-1}$ dissolved in toluene was spin-coated at a speed of 4,000 RPM for 35 s and then annealed at 100 °C for 10 min. Before depositing perovskite films, the PTAA film was pre-wetted by spinning 80 µl DMF at 4,000 RPM for 15 s to improve the wetting property of the perovskite precursor solution. The perovskite precursor solution composed of mixed cations (lead (Pb), cesium(Cs), formamidinium (FA) and methylammonium (MA)) and halides (I, Br) was dissolved in mixed solvent (DMF/DMSO = 4:1) with a chemical formula of $Cs_{0.05}FA_{0.81}MA_{0.14}PbI_{2.55}Br_{0.45}$. Then 80 µl precursor solution was spun at 2000 RPM for 2 s and 4000 RPM for 25 s, and the film was quickly washed with 130 µl toluene at 20 s during spin-coating. The sample was annealed at 65 °C and 100 °C each, for 10 min. The devices were finished by thermally evaporating C60 (30 nm), BCP (8 nm) and copper (140 nm) in sequential order.

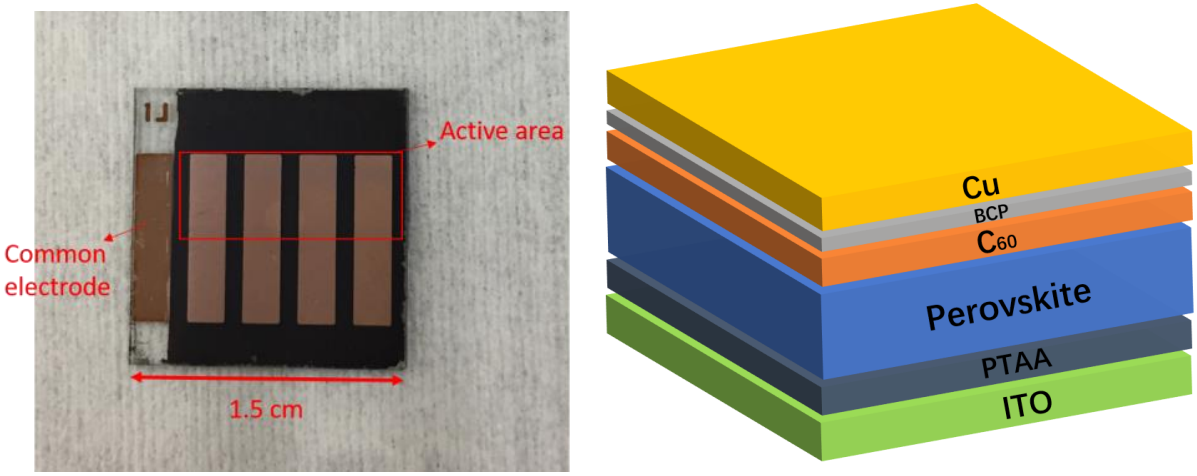


*Figure 2: (a) Top View of a PSC sample (without a ITO glass) (b) Device Structure of P-i-n PSC*

### Radiation stability in-situ irradiation measurement

The in-situ experiment was conducted utilizing the $^{137}$Cs irradiator benchtop. The gamma-ray irradiator provided a dose rate of 1.5 krad·h$^{-1}$ to the devices. The devices were positioned at the center of the benchtop in a fixed location. A solar simulator produced simulated AM1.5G illumination on the devices with constant light density of 49.8 W·m$^{-2}$ via light fiber (Light Source: Ocean Optics HL-2000-HP, Fiber: Ocean Optics QR600-7-UV-125F, Lens: Ocean Optics 74-UV). All devices were measured by a Keithley 2612A Source-Meter with scan rate of 0.017 V·s$^{-1}$. The cells were connected to the source-meter near the benchtop with a triaxial cable. A computer connected to the Keithley system source-meter via ethernet was used to control the source-meter to conduct I-V characterization at certain time interval and save the data in the local disk. The experimental environment was maintained at room temperature (23 ± 2 °C). Using this setup, the perovskite solar cell devices were characterized in-situ while being subjected to the simulated AM1.5G illumination and gamma-ray irradiation. Fig.3 shows the in-situ experimental setup.

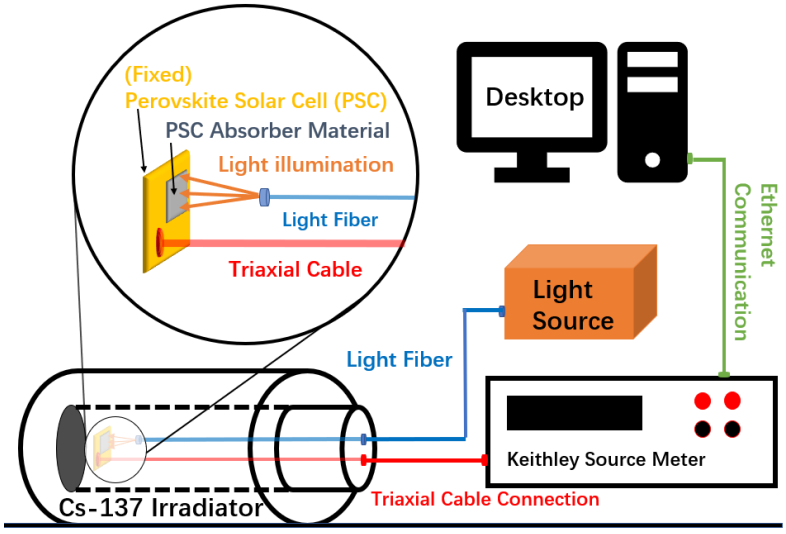


*Figure 3: Schematic of the in-situ measurement for PSC inside the $^{137}$Cs irradiator*

### Post-irradiation characterization

The morphology and structure of the samples were characterized by Quanta 200 FEG environmental scanning electron microscope. The J-V analysis of solar cells was performed using a solar light simulator (Oriel 67005, 150 W Solar Simulator) and the power of the simulated light was calibrated to 100 $mW \cdot cm^{-2}$ by a silicon (Si) diode (Hamamatsu S1133) equipped with a Schott visible-color glass filter (KG5 color-filter). All cells were measured using a Keithley 2400 Source-Meter with a scan rate of 0.1 $V \cdot s^{-1}$. External quantum efficiency curves were characterized with a Newport QE measurement kit by focusing a monochromatic beam of light onto the devices. The tDOS of solar cells were derived from the frequency-dependent capacitance (C-f) and voltage dependent capacitance (C-V), which were obtained from the TAS measurement performed by a LCR meter (Agilent E4980A).

# Results and Discussion

### Measurement of dose rate on PSC samples

The dose rate and accumulative dose of perovskite devices received inside a $^{137}Cs$ irradiator was estimated from its initial dose rate following the decay law and also validated by vendor read dosimeter (LANDAUER nanoDot$^{@}$). The dose rate at the beginning of the experiment (April 2017) was 1.92 $krad \cdot h^{-1}$. To accurately estimate the dose at the location of our perovskite solar cell devices, the dosimeter was placed at the same spot where the devices were held during the in-situ tests. Two measurements were performed, and the results are shown in **Table 1**. The dose rate at where the devices were irradiated is measured as 1.5 Krad $h^{-1}$.

*Table 1: Measurement results of nanoDot*

| NanoDot | Irradiated Time (min) | Dose Amount (cGy) |
|---|---|---|
| #1 | 15.0 | 347.74 |
| #2 | 31.0 | 801.48 |

## Photocurrent induced by gamma irradiation

Gamma rays are high-energy photons arising from radioactive decay of atomic nuclei. When gamma rays interact with the PSCs, three types of interactions will occur. [14] For low-energy gamma photons (<50 KeV), the dominant interaction is the photoelectric (PE) effect. In this case, a gamma photon will transfer all the energy to an atomic electron and eject this electron from the atom. PE is the mechanism how a solar cell generates photocurrent under solar light. For mid-energy gamma photons (>100 KeV), the dominant interaction is the Compton Scattering (CS) effect where gamma photons lose partial energy to cause the ejection of electrons. For high-energy gamma photons (>1.02 MeV), the pair production effect is likely to occur. In this interaction, 1.02 MeV of the energy of the gamma photons will be converted into an electron-positron pair and move oppositely due to the conservation of momentum.

In this experiment, the gamma photons generated by $^{137}$Cs irradiator have the energy of 0.6617 MeV. Such gamma ray will undergo CS effect as the principal interaction, and generate free electrons via ejection from the atom. However, free electrons with high energy hardly contribute to the photocurrent because they can easily escape from the surface when there is only a low bias applied on the PSC device. Besides, the high-energy gamma rays penetrate deeply into the matter and thus only a very small portion of gamma photons can be captured by the perovskite materials. The experiment results agree with our expectation. No obvious photocurrent was

detected when we provided the PSC devices with gamma irradiation only. Figure 4 shows the photocurrent generation with the control of gamma radiation under no light illumination.

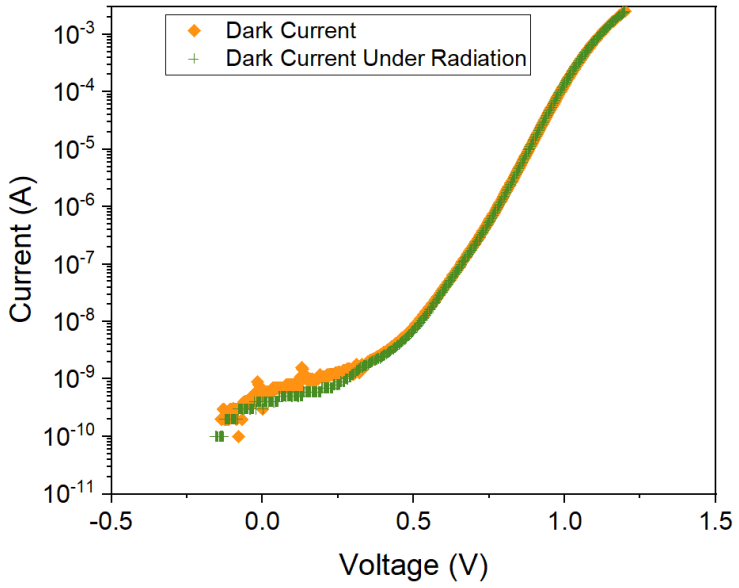


*Figure 4: I-V characteristics of a PSC sample in logarithmic scale under light-tight environment, compared between the existence of* $^{137}$Cs *gamma radiation*

## Comparison experiment between p-i-n and n-i-p PSC devices

Thin-film PSC devices differ in the structure of stacking layers. As for a typical p-i-n solar cell, the major absorbing layer is the i-layer and the n+ and p+ regions play a role in the collection of electrons and holes, respectively. Experiments were carried out to measure the performance variance of multiple p-i-n and n-i-p PSC devices for comparison. The results are shown in Table 2. PSC devices with n-i-p structure showed obvious degradation exceeding 35% in PCE after 200-hour gamma radiation. In contrast, for p-i-n PSC devices, an average radiation time of 80 h gave no degradations and in some cases there is even a slight increase in PCE.

*Table 2: The PCE after gamma radiation for PSC samples with p-i-n and n-i-p structure*

| Type | Sample Number | Radiation Time/ hour | Changes in PCE after radiation/ % |
|---|---|---|---|
| p-i-n | 1 | 90 | 2 |
| | 2 | 70 | 7.5 |
| | 3 | 90 | 6.5 |
| | 4 | 70 | 9.3 |
| n-i-p | F | 200 | -37.5 |
| | H | 170 | -36.1 |

As shown in Figure 5, it is noticed that the increase in performance for p-i-n devices is mainly caused by the change of FF. The FF of the device dropped rapidly in the first 24 h. However, the FF recovered and even enhanced with further test. The possible mechanism is analyzed in the following text.

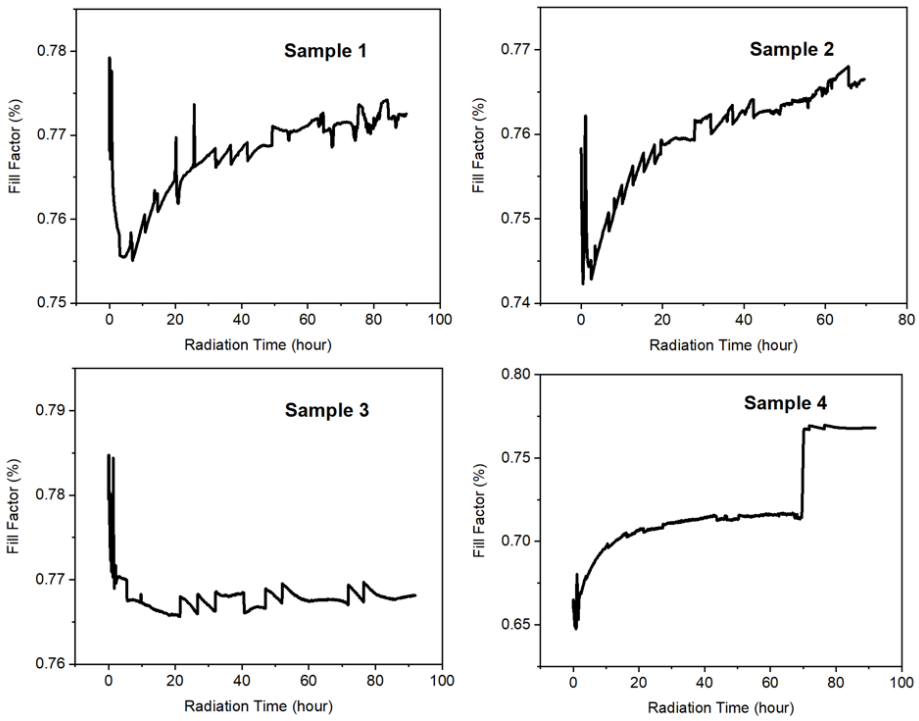


*Figure 5: Fill Factor (%) versus Radiation Time (hour) for four p-i-n PSC samples*

### Radiation stability of p-i-n PSC under long-term gamma-ray irradiation

A p-i-n PSC device was exposed to continuous light and gamma-ray radiation for over 1,535 h with a total radiation dose of 2.3 Mrad. The light intensity and radiation dose rate are measured to be 49.8 $W \cdot m^{-2}$ and 1.5 $krad \cdot h^{-1}$, respectively. As shown in Figure 6a , the PCE initially reduced to 72% in the first 24 h and then remained stable for up to 1000 h. The initial loss in PCE is relevant to the change of FF. The FF reduced to 80% in the first 24 h and recovered with further radiation test to ~95-97% after 1400 h. Similar change of FF was already observed in the earlier comparison experiment. Both the short-circuit current density ($J_{SC}$) and open-circuit voltage ($V_{OC}$), are gradually reduced to ~84-85%, respectively, of the original value by the end of the test. There are some noise in the FF and PCE metrics after testing for 960 h. It is suggested that the abnormal noise comes from the malfunction of electrical contacts.

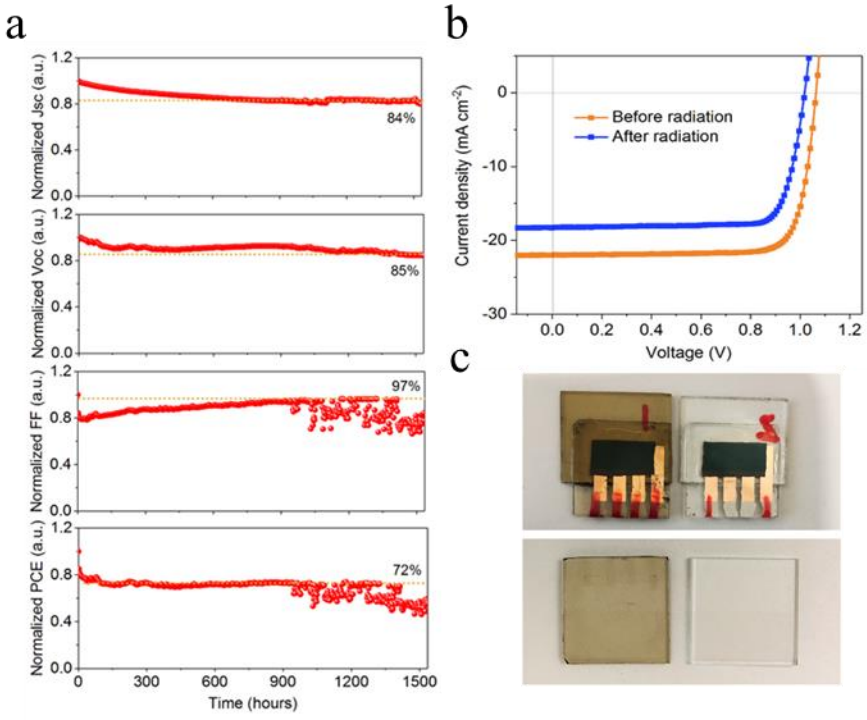


*Figure 6. (a) Radiation stability of an encapsulated perovskite device. (b) J-V curves of the perovskite device before and after irradiation test (c) The color of ITO glass before and after irradiation*

The color of ITO glass significantly changed after gamma-ray irradiation, changing from colorless to dark brown given a radiation dose of 2.3 Mrad (Figure 6c). Therefore, the performance of the device is underestimated owing to the transmittance loss of the darkened ITO glass. ITO glass is a semiconductor material with a band gap of ~4 eV. Such large band gap makes ITO mostly transmittable to photons in the visible light region and thus appears to be optically transparent. [15] Gamma rays interact with ITO glass by ionization and displacement of atoms. Irradiated by high-energy gamma rays, the perovskite materials may experience the displacement of atoms due to recoil inside their semiconductor structure, leaving lattice defects and forming energy levels within the band gap. The intermediate energy levels serve as trapping and recombination centers. [15] With energy levels introduced, photons with energy lower than the initial band gap may be captured and gradually narrow down the optical band gap. Consequently, the transmittance of ITO glass decreases in the visible light region, especially on the low-wavelength side, and hence gradually presents a darkened color.

Dr. Huang and his group measured the UV-vis vis transmittance spectra of the ITO substrates before and after irradiation to qualify the light loss and the results are shown in Figure 7. The transmittance of ITO glass reduced from ~90% over the entire visible light range to ~50-75% after irradiation. The loss of incident light is mainly centered at about 420 nm with a peak value of ~24.5%. By calculating the optical transmittance and external quantum efficiency (EQE), the irradiance level of the light source incident on the samples was found to retain 84.1% of the original value. As the $I_{SC}$ is proportional to incident light intensity [16], the loss in short-circuit current caused by darkened ITO glass is ~84% as well.

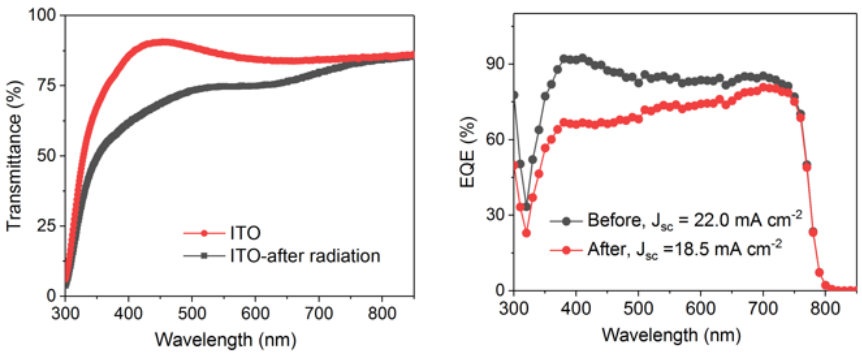


*Figure 7: (a) The transmittance (%) and (b) External Quantum Efficiency (%) of ITO glass before and after radiation*

Table 3 shows that the $J_{SC}$, $V_{OC}$, FF, and PCE of PSCs about the radiation damage in a tabular form. A correction of the transmittance loss on ITO glass is applied. It shows that this PSC device retains 94.6% of its PCE given a total radiation dose of 2.4 Mrad.

*Table 3:* Photovoltaic parameters of a perovskite device before and after gamma-ray irradiation

| | $J_{SC}$/mA $cm^{-2}$ | $V_{OC}$/V | FF | PCE/% |
|---|---|---|---|---|
| Before irradiation | 21.98 | 1.06 | 0.805 | 18.77 |
| After irradiation | 18.18 | 1.02 | 0.802 | 14.95 |
| After radiation corrected | 21.71 | 1.02 | 0.802 | 17.76 |

The primary effect of high energy radiation on solar cells is displacement damage where atoms in the semiconductor lattice are removed from their equilibrium position. When it comes to high-energy gamma ray, [17] The displacement is caused by the recoil of atoms along with the ejection of outer shell electrons, which form point defects in the crystal lattice of solar cells. These defects would induce energy levels within the forbidden gap of the active layer as charge trapping sites, and thereby degrade the electrical parameters, such as diffusion length, carrier lifetime, etc. [18] Perovskite is a highly ionic material with ease of ion migration. The occurrence of the ion movement reduces the performance in the initial 24 h. The time scale is also in accordance with

previous reports about ion migration in perovskites. Then, the maximum output in Figure 6b is almost unchanged during 100-1300 h. If we consider the light loss and gradually reduced $J_{SC}$ from the ITO substrate, we can conclude that the real PCE would be enhanced and partially recovered in this period. The self-healing capacity of perovskite can be explained by their low formation energy and ease of ion migration that the escaped or interstitial ions more easily refill the vacancies.[19] In contrast, the photovoltaic materials, such as crystalline-Si, with high formation energy are scarcely reported to have the self-healing effect.

Figure 8a showed the dark current curves of a standard PSC device (control) and the irradiated one. Both devices exhibit small leakage current density lower than 10 $mA \cdot cm^{-2}$ even under a large reverse bias of 2 V, implying that gamma-ray irradiation has not caused leakage current by forming pin-holes or ionic defects. Dr. Huang and his group further conducted thermal admittance spectroscopy (TAS) to quantitatively probe the change trapping states in the devices. Figure 8b shows that the device after irradiation has the similar trap density of states (tDOS) between ~$10^{16}$-$10^{18}$ $m^{-3} \cdot eV^{-1}$ almost over the entire trap depth region. The trap bands are classified into three as labeled in the figure (separated by orange dotted lines). The density of shallower trap states (band 1) of the irradiated device is a little larger, less than one order of magnitude compared with the control device, whereas the trap states in bands 2 and 3 are closer to that of the control sample. Results from device characterization indicate that the gamma-ray radiation does not form trap states by introducing crystal point defects.

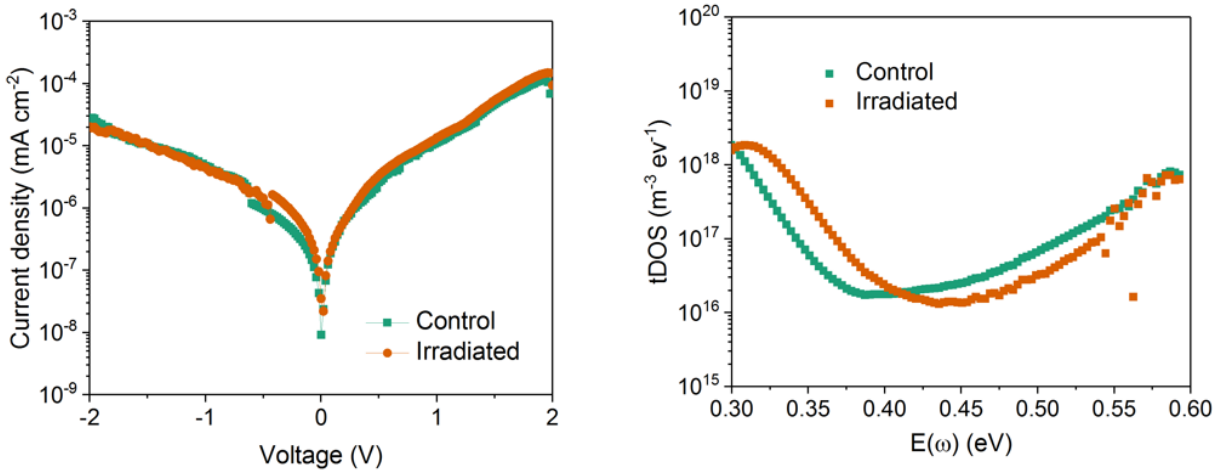


*Figure 8: (a) The dark current density (mA/cm$^{-2}$) versus voltage (V) between irradiated and control PSC devices (b)The trap density between irradiated and control PSC devices*

# Conclusion

In this paper, we discussed the effect of gamma-ray irradiation on the J-V characteristics of solar cell devices based on organohalide lead perovskite. The solar cell devices are placed inside a $^{137}$Cs irradiator benchtop with continuous exposure to gamma-ray radiation and simulated AM1.5G illumination for a total time of 1535 h and total dose of 2.3 Mrad. The light density and dose rate are estimated to be 49.8 W·m$^{-2}$ and 1.5 krad·h$^{-1}$, respectively. During the irradiation, the PCE of our device reduced to about 72% in the first 24 h and then remained stable up to 1000 h. After correction of the transmittance loss of ITO glass caused by gamma-ray radiation, the perovskite is found capable of self-healing and the FF recovered to 95%-97% at 1400 h. The post-irradiation measurement demonstrates the resistance of perovskite solar cells to high-energy gamma-ray radiation in the long run. The perovskite solar cells retained their PCE at 94.6%, compared to the 61.2% of silicon cells under similar irradiation conditions. TAS performed on

the irradiated device indicates that no intermediate energy levels and trap states were introduced by gamma rays, which reflects a higher radiation stability than the ITO glass.

# Acknowledgement

This research was funded by Defense Threat Reduction Agency (DTRA). We thank for the staff of The Ohio State University Nuclear Reactor Laboratory for their support. We thank for Dr. Huang and his group at the University of North Carolina at Chapel Hill for the fabrication of Perovskite solar cells and the post-irradiation measurements on irradiated solar cells. Due to their contribution, Dr. Huang and his group will be the authors of a paper to be submitted. We thank Xue Sha for her contribution in conducting the early experiment, experiment setup, and data analysis. We thank the college of engineering at the Ohio State University for their scholarship support.

# References

[1] M. Green, A. Ho-Baillie and H. Snaith, "The emergence of perovskite solar cells", Nature Photonics, vol. 8, no. 7, pp. 506-514, 2014.

[2] A. Kojima, K. Teshima, Y. Shirai and T. Miyasaka, "Organometal Halide Perovskites as Visible-Light Sensitizers for Photovoltaic Cells", Journal of the American Chemical Society, vol. 131, no. 17, pp. 6050-6051, 2009.

[3] W. Yang, B. Park, E. Jung, N. Jeon, Y. Kim, D. Lee, S. Shin, J. Seo, E. Kim, J. Noh and S. Seok, "Iodide management in formamidinium-lead-halide–based perovskite layers for efficient solar cells", Science, vol. 356, no. 6345, pp. 1376-1379, 2017.

[4] T. Berhe, W. Su, C. Chen, C. Pan, J. Cheng, H. Chen, M. Tsai, L. Chen, A. Dubale and B. Hwang, "Organometal halide perovskite solar cells: degradation and stability", Energy & Environmental Science, vol. 9, no. 2, pp. 323-356, 2016.

[5] J. Christians, P. Schulz, J. Tinkham, T. Schloemer, S. Harvey, B. Tremolet de Villers, A. Sellinger, J. Berry and J. Luther, "Tailored interfaces of unencapsulated perovskite solar cells for >1,000 hour operational stability", Nature Energy, vol. 3, no. 1, pp. 68-74, 2018.

[6] B. Qi and J. Wang, "Fill factor in organic solar cells", Physical Chemistry Chemical Physics, vol. 15, no. 23, p. 8972, 2013.

[7] N. Scarratt, J. Griffin, T. Wang, Y. Zhang, H. Yi, A. Iraqi and D. Lidzey, "Polymer-based solar cells having an active area of 1.6 cm2 fabricated via spray coating", APL Materials, vol. 3, no. 12, p. 126108, 2015.

[8] D. Gupta, M. Bag and K. Narayan, "Correlating reduced fill factor in polymer solar cells to contact effects", Applied Physics Letters, vol. 92, no. 9, p. 093301, 2008.

[9] F. Lang, N. Nickel, J. Bundesmann, S. Seidel, A. Denker, S. Albrecht, V. Brus, J. Rappich, B. Rech, G. Landi and H. Neitzert, "Radiation Hardness and Self-Healing of Perovskite Solar Cells", Advanced Materials, vol. 28, no. 39, pp. 8726-8731, 2016.

[10] Y. Miyazawa, M. Ikegami, T. Miyasaka, T. Ohshima, M. Imaizumi and K. Hirose, "Evaluation of radiation tolerance of perovskite solar cell for use in space", 2015 IEEE 42nd Photovoltaic Specialist Conference (PVSC), 2015.

[11] K. Motoki, Y. Miyazawa, D. Kobayashi, M. Ikegami, T. Miyasaka, T. Yamamoto and K. Hirose, "Degradation of CH3NH3PbI3 perovskite due to soft x-ray irradiation as analyzed by an x-ray photoelectron spectroscopy time-dependent measurement method", Journal of Applied Physics, vol. 121, no. 8, p. 085501, 2017.

[12] E. Benton and E. Benton, "Space radiation dosimetry in low-Earth orbit and beyond", Nuclear Instruments and Methods in Physics Research Section B: Beam Interactions with Materials and Atoms, vol. 184, no. 1-2, pp. 255-294, 2001.

[13] H. Wei, D. DeSantis, W. Wei, Y. Deng, D. Guo, T. Savenije, L. Cao and J. Huang, "Dopant compensation in alloyed CH3NH3PbBr3−xClx perovskite single crystals for gamma-ray spectroscopy", Nature Materials, vol. 16, no. 8, pp. 826-833, 2017.

[14] K. Scharf, "Photovoltaic effect produced in silicon solar cells by x-rays and gamma rays", Journal of Research of the National Bureau of Standards Section A: Physics and Chemistry, vol. 64, no. 4, p. 297, 1960.

[15] A. Alyamani and N. Mustapha, "Effects of high dose gamma irradiation on ITO thin film properties", Thin Solid Films, vol. 611, pp. 27-32, 2016.

[16] M. Liu, M. Endo, A. Shimazaki, A. Wakamiya and Y. Tachibana, "Light Intensity Dependence of Performance of Lead Halide Perovskite Solar Cells", Journal of Photopolymer Science and Technology, vol. 30, no. 5, pp. 577-582, 2017.

[17] M. Yamaguchi, C. Uemura and A. Yamamoto, "Radiation damage in InP single crystals and solar cells", Journal of Applied Physics, vol. 55, no. 6, pp. 1429-1436, 1984.

[18] Y. Yuan and J. Huang, "Ion Migration in Organometal Trihalide Perovskite and Its Impact on Photovoltaic Efficiency and Stability", Accounts of Chemical Research, vol. 49, no. 2, pp. 286-293, 2016.

[19] J. Huang, Y. Yuan, Y. Shao and Y. Yan, "Understanding the physical properties of hybrid perovskites for photovoltaic applications", Nature Reviews Materials, vol. 2, no. 7, p. 17042, 2017.